

FORMATION PROCESS AND CHARACTERIZATION OF SPHERE-LIKE BACTERIAL CELLULOSES IN AGITATED CULTURE IN TWO DIFFERENT MEDIA

JICAI BI,^{*,**} SIXIN LIU^{**,***} and CONGFA LI^{**}

^{*}School of Food Science and Technology, Henan Institute of Science and Technology, Xinxiang, 453003, China

^{**}College of Food Science and Engineering, Hainan University, Haikou 570228, China

^{***}College of Science, Hainan University, Haikou 570228, China

✉ Corresponding authors: S. Liu, sixinliu@126.com

C. Li, congfa@vip.163.com

Received January 19, 2020

The formation process of sphere-like bacterial cellulose was investigated using *Komagataeibacter nataicola* Y19 in agitated culture in Hestrin-Schramm medium (HS) and fermented coconut water medium (FCW), and the BC particles obtained were characterized. Two kinds of BCs were obtained, and their morphology changed from filamentous BC on the 1st day to final solid sphere-like BC on the 7th day, and accordingly, the size of internal pores decreased gradually, the degree of crystallinity increased gradually from 76.44% to 84.23% (HS) or from 62.11% to 79.53% (FCW), I_a decreased gradually from 76.63% to 70.84% (HS) or from 70.69% to 55.74% (FCW) and I_b increased gradually, the thermal stability increased and the maximum decomposition temperature (T_{max}) rose from 316.92 °C to 339.08 °C (HS) or from 305.07 °C to 334.44 °C (FCW).

Keywords: sphere-like bacterial cellulose, formation process, agitated culture, Hestrin-Schramm medium, fermented coconut water medium, *Komagataeibacter nataicola*

INTRODUCTION

Cellulose is a very important and fascinating biopolymer, and an almost inexhaustible and sustainable natural polymeric raw material,¹ which is of special importance both to industries and in our daily life. It is an important structural component of the primary cell wall of green vascular plants, consisting of a linear homopolysaccharide containing several hundred to over ten thousand repeating units of D-glucose linked together with a β-1,4 linkage.² Cellulose could also be secreted by *Komagataeibacter*, *Gluconacetobacter*, *Rhizobium*, *Agrobacterium*, *Rhodobacter* and *Sarcina*.²⁻⁴

As bacterial cellulose exhibits several unique properties, such as high mechanical strength, high crystallinity, high water absorption capacity, high porosity, high purity, moldability, biodegradability and excellent biological affinity, an increasing number of researchers have focused on its applications in various fields in recent years. The water uptake of BC is significant, it can absorb more than 99% water. Due to its properties, BC has been investigated for a variety of applications, such as in acoustic transducer diaphragms, paper manufacturing, filtration, pharmaceutical applications, food applications, electrically conductive materials *et al.*^{2,5-10}

Sphere-like BC has a wide application prospect due to its regular shape, large specific surface area and no need for mechanical cutting. It can be produced in agitated culture, but this has caused many problems, such as the accumulation of cellulose-negative (Cel⁻) mutants,¹¹ non-Newtonian viscosity behavior and insufficient oxygen supply during BC production.¹²⁻¹⁴ Despite these problems, the agitated culture might be the most suitable technique for large scale production.^{5,15} In our laboratory, we obtained a series of BC with unique solid sphere-like structures, synthesized by a specific strain – *Komagataeibacter nataicola* Y19. Despite previous research, the formation process of sphere-like BC grown from micro-fibre to big solid sphere-like BC remains unclear. In the present study, the formation process of sphere-like bacterial cellulose was investigated using *K. nataicola* Y19 in Hestrin-Schramm medium (HS) and fermented coconut water medium (FCW) in agitated culture, and the BC particles obtained were characterized.

EXPERIMENTAL

Micro-organisms, media and fermentation conditions

K. nataicola Y19 was used in the study and stored in the Lab of Applied Microbiology, College of Food Science and Technology, Hainan University. Hestrin-Schramm (HS) medium¹⁶ with pH adjusted to 6.0 and fermented coconut water (FCW) medium (3 g/L (NH₄)SO₄, 0.3 g/L MgSO₄, 0.3 g/L KH₂PO₄, 70% v/v fermented coconut water, sugar adjusted to 5 °Brix, pH adjusted to 4.0) were added with Congo red, which was used as an indicator for bacterial cellulose generation in HS and FCW, and could provide the label for a rapid growth of sphere-like BC.¹⁷ The main cultures were grown in a 200 mL Bunsen beaker at rotational speeds of 130 rpm (our previous experiments had shown that sphere-like BC can be stably produced at this speed) for 7 days at 30 °C. The synthesized cellulose was separated by filtration and washed with 1% sodium hydroxide solution to remove the cells and the media, followed by washing with distilled water till pH 7.

Analysis of properties of bacterial cellulose

Freeze-dried bacterial cellulose samples were coated with platinum and viewed under a scanning electron microscope in the usual way (S-3000n, Hitachi, Japan).¹⁸⁻²⁰

Iα mass fractions were calculated using absorbency data from recorded FTIR spectra (256 scans, 2 cm⁻¹ in the range from 4000 to 400 cm⁻¹). The following formula described by Yamamoto *et al.* was used in calculations:²¹ $f_\alpha = 2.55f_\alpha^{IR} - 0.32$, where f_α^{IR} of cellulose can be calculated as $A_\alpha/(A_\alpha + A_\beta)$, where A_α and A_β are absorbencies at 750 cm⁻¹ and 710 cm⁻¹, respectively.

The crystal structure of the bacterial cellulose samples was analyzed by an X-ray diffractometer (D8-Advance, Bruker AXS) at ambient temperature, using Cu K α (1.5406 Å) radiation between $2\theta = 5^\circ - 60^\circ$ at 1 second step size and increment of 0.01 degree with 0.5° or 1.0 mm of divergent and anti-scattering slit. The relative crystallinity index was calculated according to the formula constructed by Segal:²² Cr I = $(I_{200} - I_{am})/I_{200}$, where I_{200} is the overall intensity of the peak at 2θ of about 22.9° and I_{am} is the intensity of the baseline at 2θ of about 18°.²³ The crystal size was calculated using the Scherrer equation:²⁴ $D_{hkl} = K\lambda/\beta_{hkl}\cos\theta_{hkl}$, where β is the breadth of the peak of a specific phase (hkl), K is a constant that varies with the method of taking the breadth (0.89 < K < 1), λ is the wavelength of incident X-rays ($\lambda = 1.5406 \text{ \AA}$), θ is the center angle of the peak, and D is the crystallite length (size).

The thermal properties of the bacterial cellulose samples were analyzed by a thermogravimetric analyzer (TGA) machine (SDT Q600, TA Instruments). The weight loss was recorded under N₂ (40 mL/min) atmosphere in the range of 50 °C and ~500 °C, at a heating rate of 10 °C/min, at which point only ashes remained.^{25,26} A weight loss curve and its derivative curve were thus obtained to determine decomposition temperatures and associated weight losses.^{27,28}

RESULTS AND DISCUSSION

Macro- and micro-morphology of BCs during culture process

Light solid sphere-like BC particles were accumulated in the agitated culture from the 1st day to 7th day (Fig. 1). Congo red could stain the cellular tissue due to its strong affinity to cellulose fibers,²⁶ and therefore it was used to observe the formation process of sphere-like BC. In addition, Congo red had no influence on the macroscopic morphology of the sphere-like BC, which was different for the two media. In HS, the sphere-like BC began to form after 24 hours in the agitated culture, with a visible fine filamentous BC being observed (Fig. 1 HS). On the 1st day, the BC looked like loose filamentous and colloidal particles, consisting of several coarse filaments as basic framework (Fig. 2 HS). Also, the smaller filamentous structure was distributed around the basic framework. On the 2nd day, BC “grew” larger and a series of non-uniform loose sphere-like BC particles formed. On the 3rd day, more sphere-like BC particles, with larger diameter, could be seen, and the original initial filamentous framework was surrounded by gelatinous BC. From the 4th to the 7th day, the sphere-like BC particles grew bigger and bigger, with the diameters of the particles being about 5-10 mm, however the number of sphere-like BC particles did not change. Meanwhile, in FCW, the BC particles observed had a diameter of 0.05-0.1 cm, of irregular point-like shape on the 1st day (Fig. 1 FCW). We also observed the formation of new “born” fiber and oval shaped bacteria surrounded by BC by dying with Congo red (Fig. 2 FCW). On the 2nd day, more punctate particles with a larger diameter, of 0.1-0.2 cm, formed, and even some clusters formed. On the 3rd day, the small particles combined into larger particles with the diameter of 0.2-0.3 cm. From the 4th day to the 7th day, the particles continued to “grow”, reaching a final diameter of 0.6-0.8 cm. Every particle was wrapped by 2-6 small particles.

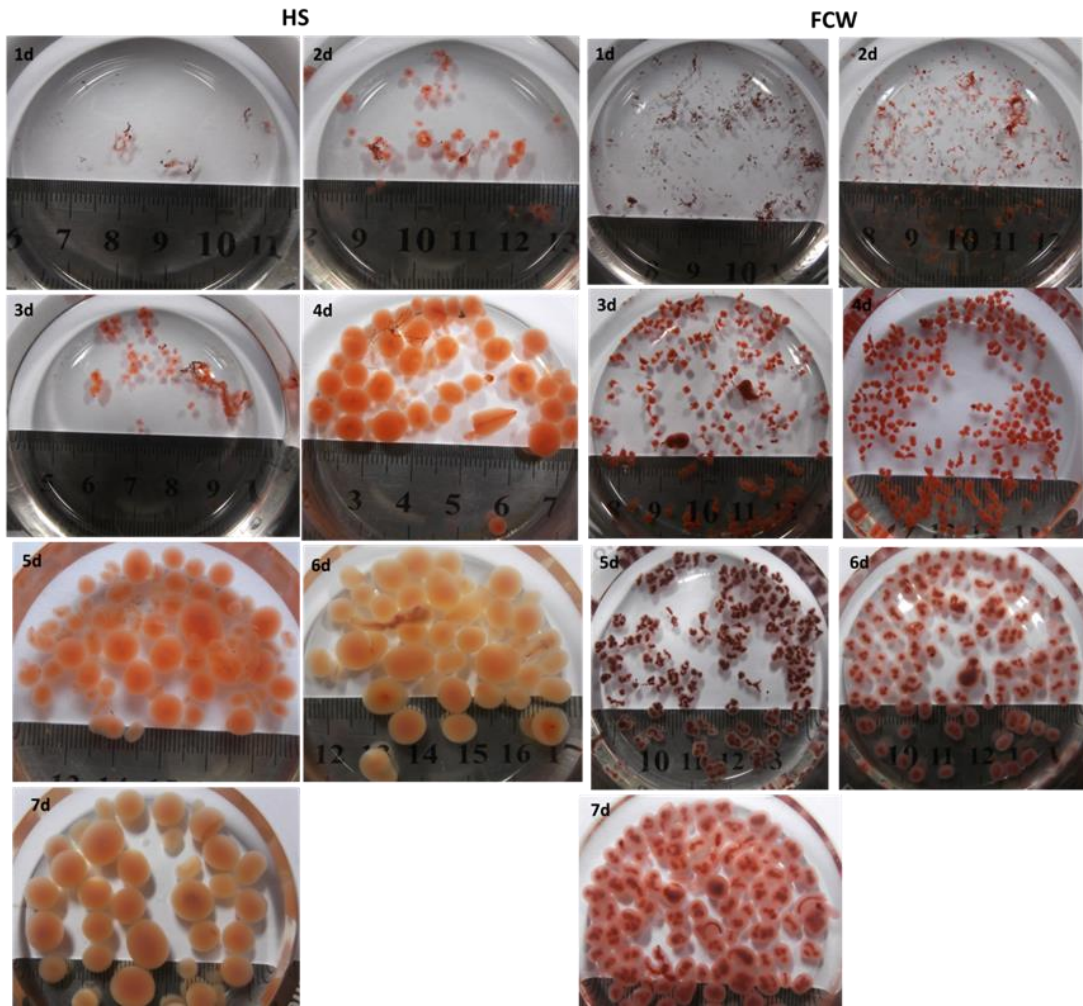


Figure 1: Optical images of BC samples prepared in agitated culture in HS (right) and FCW (left) media from the 1st to the 7th day with Congo red staining

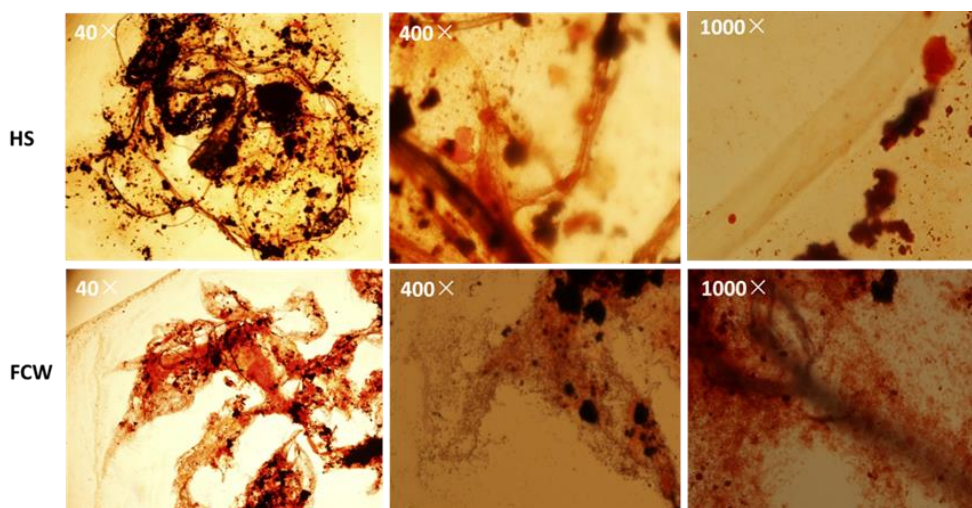


Figure 2: Optical microscopic observation of filamentous BC prepared in agitated HS (above) and FCW (below) media on the 1st day with Congo red staining

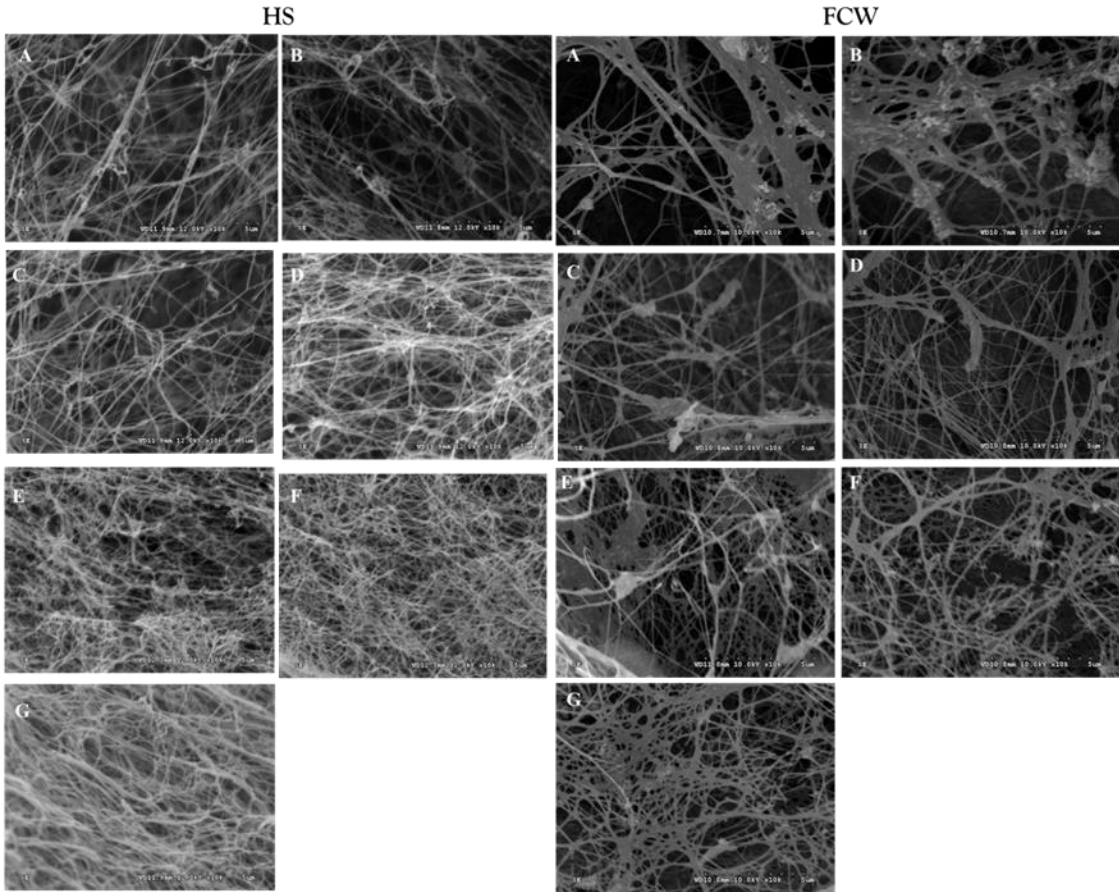


Figure 3: SEM images of BC samples without Congo red prepared in agitated culture in HS (right) and FCW (left) media, from day 1 to day 7 (A to G, respectively)

In order to observe the BC microfibrils, SEM images were obtained. Our results illustrated a disordered reticulated structure, consisting of ultrafine fibrils of 50-100 nm width. The width of the ultrafine fibrils produced during the culture process was almost the same. In HS medium (Fig. 3 HS), filamentous BC on the 1st day was the loosest and largest in terms of pore size, while the solid sphere-like BC of the 7th day was the most compact and with the smallest pore size. SEM results illustrate that, from day 1 to day 7, the fiber bundles became more and more compact, while the pore size reduced gradually. Based on the observations mentioned above, the sphere-like BC became larger in diameter and more compact, with reduced pore size along the culture process. As for FCW (Fig. 3 FCW), the filamentous BC under SEM observation on day 1 to day 2 showed loosely arranged fiber bundles, with larger pore size. The fiber bundles were intertwined. From day 3 to day 7, the number of the fiber bundles increased, while the pore diameter and the degree of adhesion reduced gradually.

We obtained two kinds of BCs and their morphology changed from filamentous on the 1st day to solid sphere-like BC on the 7th day, and accordingly, the size of internal pores decreased gradually. Sheykhanzari *et al.* used *Gluconacetobacter xylinus* BPR 2004 to investigate the effects of growth time on BC structure.²⁹ They found that increasing the growth time up to 7 days could improve the number of microfibril branches crossing to each other. The number of bundles increased, while further prolonging the growth time up to 21 days led to weaker microfibrils network.²⁹ The BC microfibrils produced in agitated culture were more twisted and curlier than those obtained in stationary culture, maybe because of the shear force of the turbulent current in agitated broth.^{30,31} The highly hydrophilic BC surface can promote a homogenous distribution of drugs within the BC membranes.³² Also, it has been observed that new modifications did not alter the existing favorable properties of solid sphere-like BC, while adding novel advantageous features to the material.³³ Thus, solid sphere-like BC was found suitable for the development of drug release materials. Unfortunately, the production cost of BC is too high, thus reducing its commercial attractiveness and limiting industrial scale production.³⁴

This research is an attempt at developing cheaper production pathways for achieving solid sphere-like BC.

X-ray diffraction analysis

Figure 4 reveals that the BCs prepared in agitated culture in HS and FCW media were the typical crystalline form of cellulose I. It is known that the crystalline structure of cellulose I is a mixture of two distinct crystalline variations: I_α meta-stable state celluloses (triclinic) and I_β stable state celluloses (monoclinic).⁵ The chemical and physical properties of cellulose had a close relation with the degree of crystallinity. A comparison of 2θ angle values (peak 1 and peak 2) revealed that the (1̄10) and (110) reflections were positioned farther over time, and they were shifted to wider angles.

The smaller value of d -spacing for the (1̄10) plane means lower I_α cellulose content in the BC. The d -spacings were of 6.23 Å, 6.07 Å, 6.00 Å, 6.03 Å, 6.02 Å, 5.96 Å and 5.92 Å for the (1̄10) plane at different time points during the preparation of BCs – from day 1 to day 7, respectively. Meanwhile, the d -spacings of BC particles produced in FCW medium were of 6.19 Å, 6.11 Å, 6.08 Å, 6.03 Å, 6.01 Å, 5.95 Å and 5.87 Å, respectively. These values suggest the cellulose I_α content in the solid sphere-like BC was lower during the course of time. The crystallite sizes and crystallinity were calculated from the (1̄10), (110) and (200) planes, using Scherrer's equation and Segal's equation, respectively (the results are listed in Table 1). The data obtained clearly demonstrate the crystallinity gradually increased from 76.44% to 84.23% (HS) and from 62.11% to 79.53% (FCW) during the course of time. It seemed that the effect of shear force on small BC particles was more intensive than on bigger solid sphere-like BC in agitated culture. This can be explained by the fact that sub-elementary fibrils in bigger solid sphere-like BC are tightly packed and stable against stronger shear force.

The supramolecular structure of cellulosic fibers could be described by a two-phase model with regions of high orientation (crystalline) and low orientation (amorphous).^{35,36} X-ray diffraction was applied to compare the crystalline structure of the BC samples.³⁷⁻³⁹ Cellulose I (natural cellulose) is the most abundant form found in nature. Miller indices for the three principal planes of reflection are (1̄10), (110), and (200) for cellulose I.⁴⁰ I_{200} is the maximum intensity of crystalline scatter at the 200 reflection (used in the case of cellulose I at $2\theta = 22.5^\circ$) and I_{am} is the intensity of diffraction at $2\theta = 18.0^\circ$ for cellulose I.⁴⁰ The degree of crystallinity increased gradually over time and the BC particles from HS had higher crystallinity than those from FCW. Gu *et al.* found that smaller elementary fibril crystals and more amorphous regions were formed under dynamic conditions.⁴¹

FT-IR spectroscopy

FT-IR spectroscopy was applied to determine the exact values of mass fractions of cellulose I_α and I_β . The FT-IR spectra of the BCs prepared in agitated culture in HS and FCW media by *K. nataicola* Y19 in the present study showed several bands typical of cellulose in the region of 1500-1250 cm⁻¹ (Fig. 5). Characteristic absorption peaks of BC were found at 3350 cm⁻¹ due to O-H stretching and at 2900 cm⁻¹ due to C-H stretching. The band at 1650 cm⁻¹ was due to the deformation vibration of the absorbed water molecules. All these characteristics of the FT-IR spectra found in the present study are indicative of bacterial cellulose. The regions of the FT-IR spectra shown in Figure 5 present peaks assigned to I_α (FT-IR absorptions at 750 cm⁻¹) and I_β (FT-IR absorptions at 710 cm⁻¹) fractions. The IR crystallinity index (CI) of BCs prepared in agitated culture in HS and FCW shown in Table 2 indicates that, on the 7th day, the BC possessed the highest CI. The I_α and I_β content (%) showed I_α decreased gradually from 76.63% to 70.84% (HS) and from 70.69% to 55.74% (FCW), and I_β increased gradually accordingly. This suggested that the macrostructure morphology changes that occurred during the course of time could influence the crystallization of cellulose sub-elementary microfibrils.

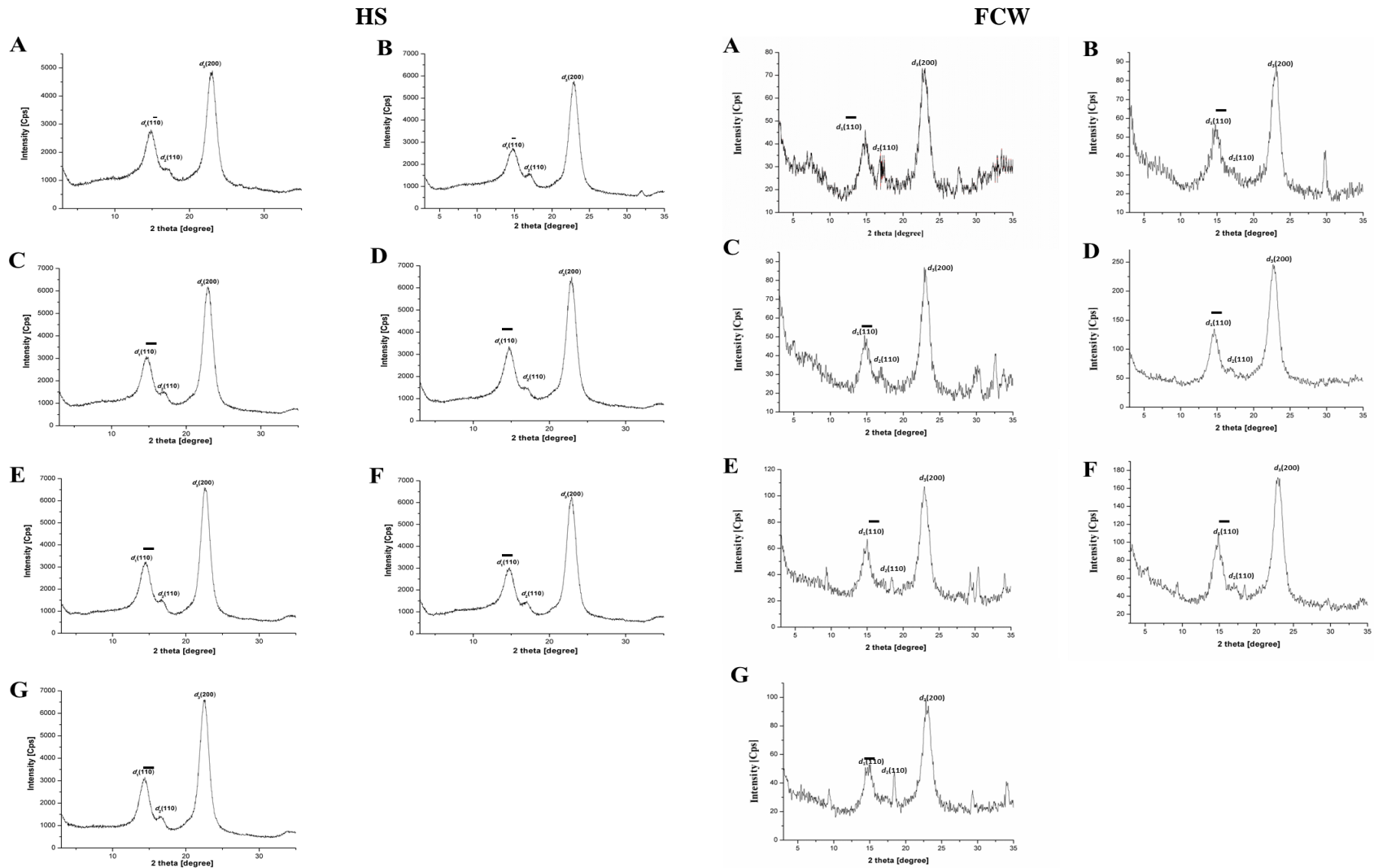


Figure 4: X-ray diffraction patterns of BCs without Congo red staining, prepared in agitated culture in HS (left) and FCW (right) media from day 1 to day 7 (A to G, respectively). Three typical diffraction peaks occurring in the region of $10\text{--}25^\circ$ were labeled as d_1 , d_2 and d_3

Table 1
D-spacings, crystallite sizes and percent crystallinity of BCs prepared in agitated culture in HS and FCW media from day 1 to day 7

BC sample	d-Spacings (Å)			Difference in 2θ angle peak1-peak2	Crystallite sizes (nm)			Percent crystallinity (%)
	<i>d</i> ₁	<i>d</i> ₂	<i>d</i> ₃		<i>cr</i> ₁	<i>cr</i> ₂	<i>cr</i> ₃	
BC-1 st day (HS)	6.23	5.18	3.86	2.151	8.2	11.4	8.4	76.44
BC-2 nd day (HS)	6.07	5.15	3.87	2.177	8.5	12.3	8.5	80.27
BC-3 rd day (HS)	6.03	5.19	3.88	2.225	8.7	13.8	8.6	81.27
BC-4 th day (HS)	6.02	5.29	3.34	2.301	8.7	14.4	8.6	81.61
BC-5 th day (HS)	6.00	5.33	3.93	2.424	8.9	14.5	8.7	82.78
BC-6 th day (HS)	5.96	5.16	3.88	2.462	8.9	14.7	8.7	83.43
BC-7 th day (HS)	5.92	5.19	3.87	2.476	9.2	15.3	8.7	84.23
BC-1 st day (FCW)	6.19	5.16	3.89	2.22	3.9	4.8	4.3	62.11
BC-2 nd day (FCW)	6.11	5.17	3.87	2.33	5.5	6.2	5	64.02
BC-3 rd day (FCW)	6.08	4.82	3.86	2.35	6.1	7.6	5.1	70.06
BC-4 th day (FCW)	6.03	5.09	3.86	2.37	7.5	10	5.8	72.14
BC-5 th day (FCW)	6.01	5.21	3.85	2.45	8	10	6	77.64
BC-6 th day (FCW)	5.95	5.25	3.91	2.53	10	11.6	7.6	78.61
BC-7 th day (FCW)	5.87	4.79	3.84	2.67	10	13.1	8.4	79.53

Table 2
Cellulose I_α and I_β contents and crystallinity index of BCs prepared in agitated culture in HS and FCW medium from 1st to 7th day

BC sample	I _α (%)	I _β (%)	IR crystallinity index (Abs. at 1428/896 cm ⁻¹)
BC-1 st day (HS)	76.63	23.37	4.23
BC-2 nd day (HS)	76.58	23.42	4.46
BC-3 rd day (HS)	74.46	25.54	4.93
BC-4 th day (HS)	72.83	27.17	5.22
BC-5 th day (HS)	72.75	27.25	5.88
BC-6 th day (HS)	71.71	28.29	6.40
BC-7 th day (HS)	70.84	29.16	6.61
BC-1 st day (FCW)	70.69	29.31	3.52
BC-2 nd day (FCW)	68.09	31.91	3.68
BC-3 rd day (FCW)	67.52	32.48	4.43
BC-4 th day (FCW)	60.51	39.49	5.04
BC-5 th day (FCW)	59.00	41.00	5.50
BC-6 th day (FCW)	56.03	43.97	6.17
BC-7 th day (FCW)	55.74	44.26	6.33

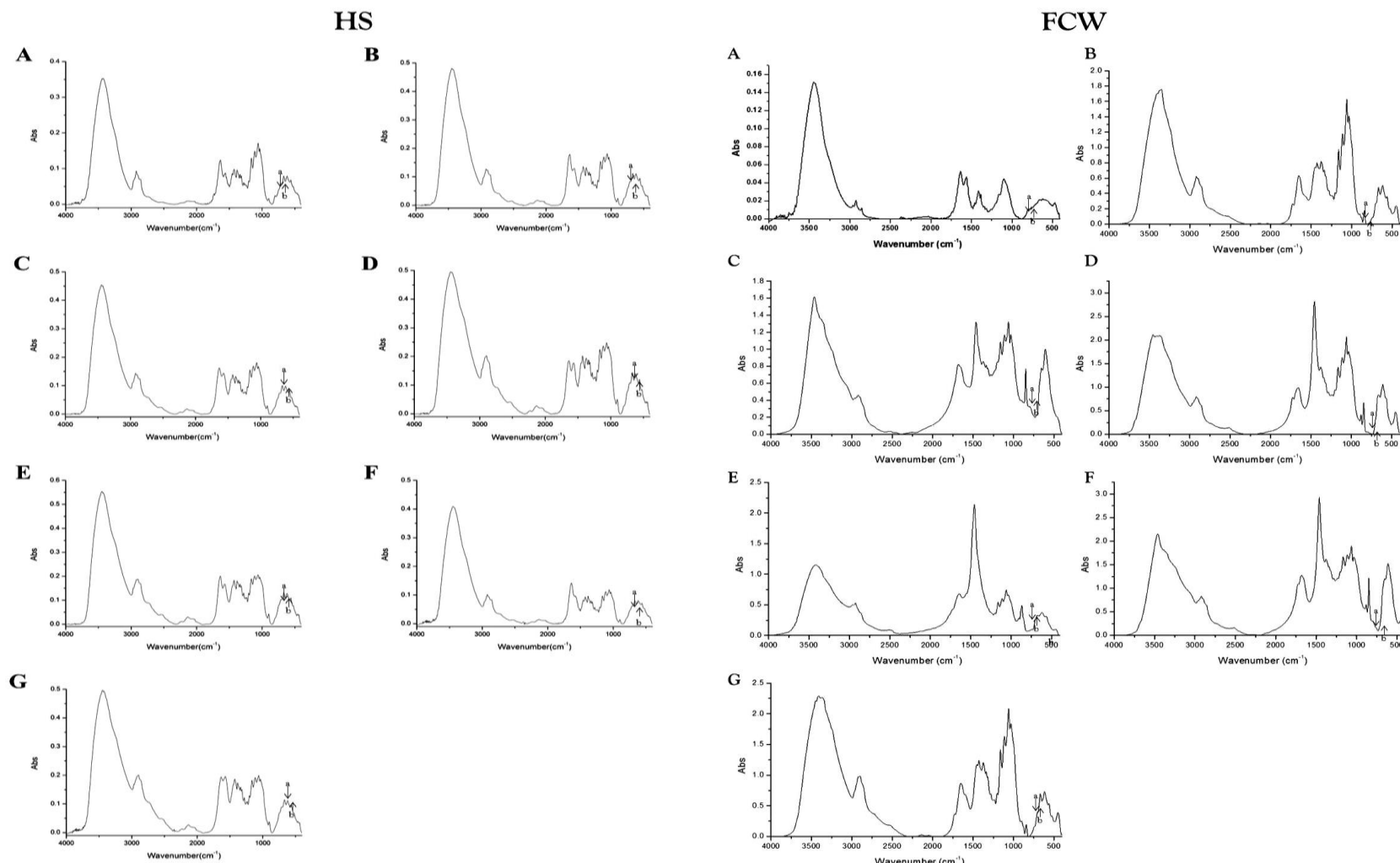


Figure 5: FT-IR spectra of BCs without Congo red staining prepared in agitated culture in HS (left) and FCW (right) media from day 1 to day 7 (A to G, respectively); I_α (a: 750 cm^{-1}) and I_β (b: 710 cm^{-1})

Sheykhanzari *et al.* found the hydrogen and C-H bonds developed with the increase in the growth time.²⁹ Our results showed the solid sphere-like BC had the same I_a mass fraction. The FT-IR results regarding the cellulose I_a content agreed with the findings of the X-ray diffraction investigation. Yamamoto *et al.* suggested that thermodynamically stable I_B cellulose was produced under less stress conditions, while the crystallization of I_a cellulose occurs under the influence of shearing stress. The grown sphere-like BC may induce a less stress condition by preventing the aggregation of microfibrils to a ribbon. The decrease of the shearing force during the process of sphere-like BC formation may be a factor for the formation of intra- and inter-molecular hydrogen bonds in sub-elementary cellulose fibrils, which disturbed their aggregation and crystallization. So, the prepared solid sphere-like BC had I_B dominant type and higher crystallinity. The content of I_a decreased gradually over time and the BC particles from HS had higher content of I_a than those from FCW. Meanwhile, the content of I_B increased gradually. Previous studies reported the production of cellulose spheres by *Acetobacter xylinum* NQ5 (ATCC 53582) in flasks at different rotational speeds (in the range of 90-250 rpm).⁴² Yan *et al.* used *Acetobacter xylinum* 1.1812 at a rotational speed of 150 rpm to obtain snow-like BC, whose I_a content was 37.46% and CI was 2.23.³⁰ Aydin *et al.* used *Gluconacetobacter hansenii* P2A to obtain a series of I_a mass fractions of 0.88, 0.81 and 0.79 for static, shaken and agitated cultivation conditions, respectively.⁴³ Several studies demonstrated that there was higher cellulose I_a content in the static culture BCs compared with that in agitated culture.^{30,43}

Thermogravimetric analysis

To determine the thermal decomposition behavior of the BCs prepared during different time periods in agitated culture, thermogravimetric analysis (TGA) was performed on the BC samples.²⁷ The maximum decomposition temperature (T_{max}), known as a criterion of thermal decomposition, was calculated from different TGA curves. Each peak on the T_{max} pattern represents the steepest slope of weight loss (%/°C) for each step during decomposition, indicating the possibility of a type of decomposition.²⁸ Figure 6 and Table 3 indicate single step degradations, with maximum decomposition temperatures of 316.92, 320.71, 322.48, 323.12, 329.77, 329.86 and 339.08 °C for the BC prepared in HS on day 1 to day 7, respectively. Meanwhile, the BCs produced in FCW medium reached maximum decomposition temperatures of 305.07, 306.68, 320.97, 325.33, 328.80, 330.02 and 334.44 °C (for day 1 to day 7, respectively).

The thermal stability increased and the maximum decomposition temperature (T_{max}) enhanced over time and the BC particles from HS reached higher values than those from FCW. Yang and Chen established that an initial weight loss at lower temperatures, ranging from 200 °C to 360 °C, can be attributed to the loss of small molecular groups, such as hydroxyl and methylhydroxyl groups.⁴⁴ The thermal degradation behavior was affected by some structure parameters, such as molecular weight, I_B content and crystallinity.⁴⁵ The thermal stability increased with the course of time, which confirmed the gradual increase in the I_B phase content and crystallinity, indicating that the achieved solid sphere-like BC possessed high thermal stability and began to degrade at higher temperature.

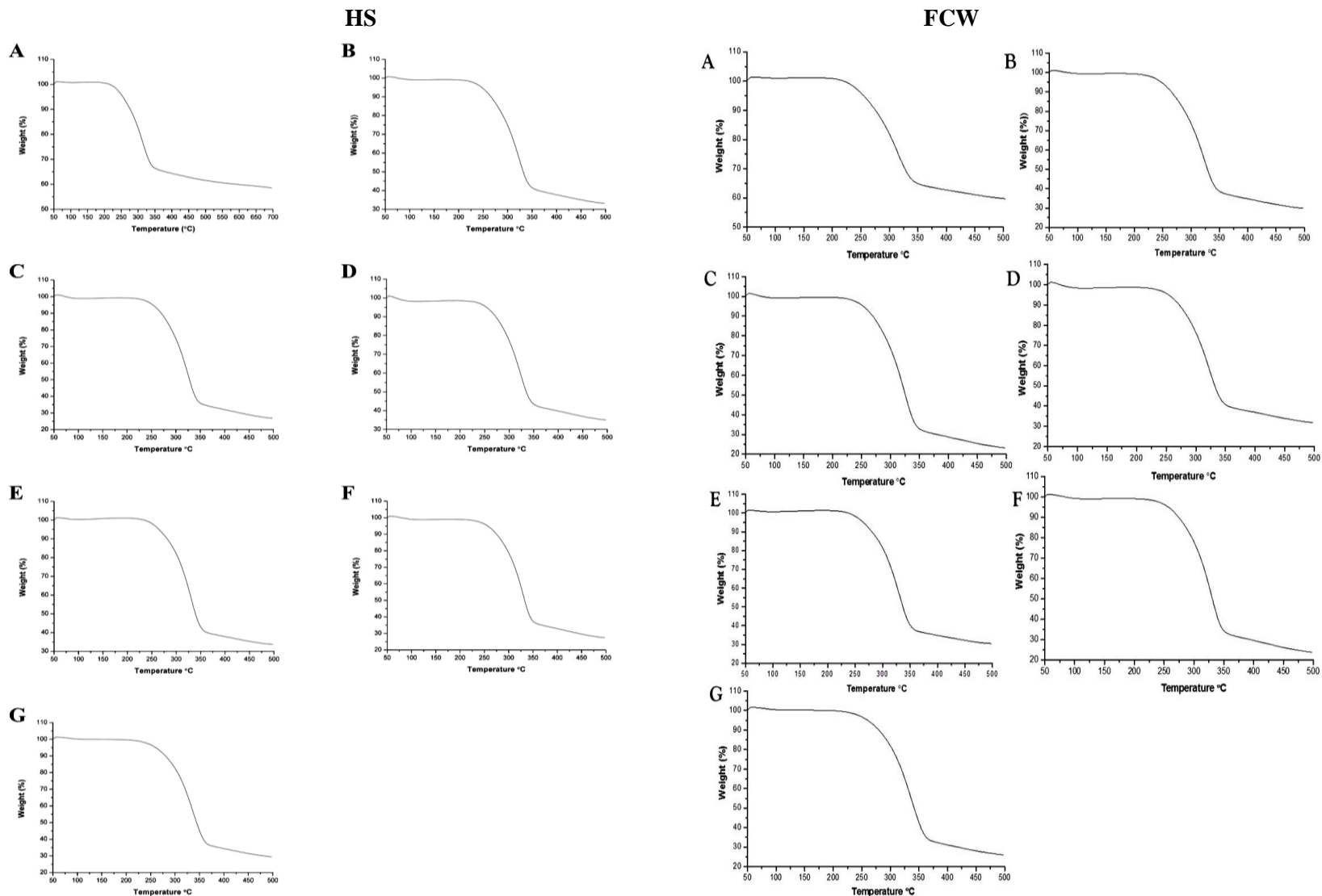


Figure 6: TGA curves of BCs without Congo red staining prepared in agitated culture in HS (left) and FCW (right) media from day 1 to day 7 (A to G, respectively)

Table 3

TGA results of BCs without Congo red staining prepared in agitated culture in HS and FCW media from day 1 to day 7

Samples	T_i (°C)	T_{max} (°C)	T_f (°C)
BC-1 st day (HS)	259.81	316.92	339.97
BC-2 nd day (HS)	274.58	320.71	341.72
BC-3 rd day (HS)	278.21	322.48	341.72
BC-4 th day (HS)	277.69	323.12	341.75
BC-5 th day (HS)	284.96	329.77	348.79
BC-6 th day (HS)	286.39	329.86	345.60
BC-7 th day (HS)	287.34	339.08	359.57
BC-1 st day (FCW)	231.66	305.07	336.67
BC-2 nd day (FCW)	232.07	306.68	352.66
BC-3 rd day (FCW)	236.07	320.97	356.73
BC-4 th day (FCW)	237.23	325.33	362.62
BC-5 th day (FCW)	241.13	328.80	367.35
BC-6 th day (FCW)	246.50	330.02	372.08
BC-7 th day (FCW)	250.76	334.44	376.97

T_i – initial temperature of decomposition; T_{max} – temperature of maximum decomposition; T_f – final temperature of decomposition

CONCLUSION

Here, we used *K. nataicola* Y19 to produce sphere-like BC in agitated culture and then characterized it. Two kinds of BCs were obtained and their morphology changed from filamentous BC on the 1st day of the formation process to final solid sphere-like BC on the 7th day. Accordingly, the size of internal pores decreased gradually, while the degree of crystallinity increased constantly from 80.44% to 88.23% (HS) or from 66.11% to 83.53% (FCW). Also, during the seven days of the formation process, the content of I_a in the BC decreased gradually from 76.63% to 70.84% (HS) or from 70.69% to 55.74% (FCW), while that of I_b increased. Finally, the thermal stability of the produced BCs increased over time and the maximum decomposition temperature (T_{max}) increased from 316.92 °C to 339.08 °C (HS) and from 305.07 °C to 334.44 °C (FCW).

ACKNOWLEDGEMENTS: This work was supported by NSFC Regional Science Foundation Project (31660458), China Special Fund for Agro-scientific Research in the Public Interest (200903026-6), as well as in part by China National Science and Technology Supporting Program Project (2007BAD76B01-2).

REFERENCES

- ¹ N. Yin, R. Du, F. Zhao, Y. Han and Z. Zhou, *Carbohyd. Polym.*, **229**, 115520 (2020), <https://doi.org/10.1016/j.carbpol.2019.115520>
- ² E. E. Brown and M. P. Laborie, *Biomacromolecules*, **8**, 3074 (2007), <https://doi.org/10.1021/bm700448x>
- ³ Y. Yamada, *Int. J. Syst. Evol. Microbiol.*, **64**, 5 (2014), <https://doi.org/10.1099/ijsm.0.054494-0>
- ⁴ X. Zou, S. Zhang, L. Chen, J. Hu and F. F. Hong, *Microb. Biotechnol.*, **13**, 458 (2019), <https://doi.org/10.1111/1751-7915.13494>
- ⁵ P. Ross, R. Mayer and M. Benziman, *Annu. Rev. Biochem.*, **84**, 95 (2015), <https://doi.org/10.1146/annurev-biochem-060614-033930>
- ⁶ N. Shah, M. Ul-Islam, W. A. Khattak and J. K. Park, *Carbohyd. Polym.*, **98**, 1585 (2013), <https://doi.org/10.1016/j.carbpol.2013.08.018>
- ⁷ V. Yadav, L. Sun, B. Panilaitis and D. L. Kaplan, *J. Tissue Eng. Regen. Med.*, **9**, E276 (2013), <https://doi.org/10.1002/term.1644>
- ⁸ C. Zhu, F. Li, X. Zhou, L. Lin and T. Zhang, *J. Biomed. Mater. Res. A*, **102**, 1548 (2013), <https://doi.org/10.1002/jbm.a.34796>
- ⁹ V. T. Nguyen, B. Flanagan, M. J. Gidley and G. A. Dykes, *Curr. Microbiol.*, **57**, 449 (2008), <https://doi.org/10.1007/s00284-008-9228-3>
- ¹⁰ C. Campano, N. Merayo, C. Negro and A. Blanco, *Int. J. Biol. Macromol.*, **118**, 1532 (2018),

<https://doi.org/10.1016/j.ijbiomac.2018.06.201>

¹¹ Y. Hu and J. M. Catchmark, *Biomacromolecules*, **11**, 1727 (2010), <https://doi.org/10.1021/bm100060v>

¹² K. Y. Lee, G. Buldum, A. Mantalaris and A. Bismarck, *Macromol. Biosci.*, **14**, 10 (2013), <https://doi.org/10.1002/mabi.201300298>

¹³ A. Tholen and A. Brune, *Environ. Microbiol.*, **2**, 436 (2000), <https://doi.org/10.1046/j.1462-2920.2000.00127.x>

¹⁴ A. C. Rodrigues, A. I. Fontao, A. Coelho, M. Leal, F. A. G. Soares da Silva et al., *New Biotechnol.*, **49**, 19 (2019), <https://doi.org/10.1016/j.nbt.2018.12.002>

¹⁵ H. Toyosaki, T. Naritomi, A. Seto, M. Matsuoka, T. Tsuchida et al., *Biosci. Biotech. Biochem.*, **59**, 1498 (1995), <https://doi.org/10.1271/bbb.59.1498>

¹⁶ S. Hestrin and M. Schramm, *Biochem. J.*, **58**, 345 (1954), <https://doi.org/10.1042/bj0580345>

¹⁷ B. V. Mohite, B. K. Salunke and S. V. Patil, *Appl. Biochem. Biotechnol.*, **169**, 1497 (2013), <https://doi.org/10.1007/s12010-013-0092-7>.

¹⁸ H. Bai, X. Wang, Y. Zhou and L. Zhang, *Prog. Nat. Sci.-Mater.*, **22**, 250 (2012), <https://doi.org/CNKI:SUN:ZKJY.0.2012-03-015>

¹⁹ J.-P. Touzel, B. Chabbert, B. Monties, P. Debeire and B. Cathala, *J. Agric. Food. Chem.*, **51**, 981 (2003), <https://doi.org/10.1021/jf020200p>

²⁰ Q. Shi, Y. Li, J. Sun, H. Zhang, L. Chen et al., *Biomaterials*, **33**, 6644 (2012), <https://doi.org/10.1016/j.biomaterials.2012.05.071>

²¹ H. Yamamoto, F. Horii and A. Hirai, *Cellulose*, **3**, 229 (1996), <https://doi.org/10.1007/BF02228804>

²² L. Segal, J. Creely, A. Martin and C. Conrad, *Text. Res. J.*, **29**, 786 (1959), <https://doi.org/10.1177/004051755902901003>

²³ A. Mihranyan, A. P. Llagostera, R. Karmhag, M. Strømme and R. Ek, *Int. J. Pharm.*, **269**, 433 (2004), <https://doi.org/10.1016/j.ijpharm.2003.09.030>

²⁴ K.-C. Cheng, J. M. Catchmark and A. Demirci, *J. Biol. Eng.*, **3**, 12 (2009), <https://doi.org/10.1186/1754-1611-3-12>

²⁵ Y. A. Aydin and N. D. Aksoy, *Appl. Microbiol. Biotechnol.*, **98**, 1065 (2013), <https://doi.org/10.1007/s00253-013-5296-9>

²⁶ J. R. Colvin and D. Witter, *Protoplasma*, **116**, 34 (1983), <https://doi.org/10.1007/BF01294228>

²⁷ K.-C. Cheng, PhD Thesis, Pennsylvania State University, 2010, p. 102, <https://etda.libraries.psu.edu/catalog/10894>

²⁸ R. Bodîrlău and C. Teacă, in *Procs. 8th International Balkan Workshop on Applied Physics*, 2009, p. 5, <https://doi.org/10.1186/s13068-016-0623X>

²⁹ S. Sheykhnazari, T. Tabarsa, A. Ashori, A. Shakeri and M. Golalipour, *Carbohyd. Polym.*, **86**, 1187 (2011), <https://doi.org/110.1016/j.carbpol.2012.05.060>

³⁰ Z. Yan, S. Chen, H. Wang, B. Wang and J. Jiang, *Carbohyd. Polym.*, **74**, 659 (2008), <https://doi.org/10.1016/j.carbpol.2008.04.028>

³¹ Y. S. Yun, H. Bak, S. Y. Cho and H. J. Jin, *J. Nanosci. Nanotechnol.*, **11**, 806 (2011), <https://doi.org/10.1166/jnn.2011.3182>

³² M. Abba, Z. Ibrahim, C. S. Chong, N. A. Zawawi, M. R. A. Kadir et al., *Fiber. Polym.*, **20**, 2025 (2019), <https://doi.org/10.1007/s12221-019-9076-8>

³³ I. Sulaeva, H. Hettegger, A. Bergen, C. Rohrer, M. Kostic, J. Konnerth and A. Potthast, *Mat. Sci. Eng.: C*, **3**, 110619 (2020), <https://doi.org/10.1016/j.msec.2019.110619>

³⁴ R. Salihu, C. Y. Foong, S. I. A. Razak, M. R. A. Kadir, A. H. M. Yusof et al., *Cellulose Chem. Technol.*, **53**, 13 (2019), <https://doi.org/10.35812/CelluloseChemTechnol.2019.53.01>

³⁵ A. Jalal Uddin, J. Araki and Y. Gotoh, *Biomacromolecules*, **12**, 617 (2011), <https://doi.org/10.1021/bm101280f>

³⁶ J. Mulligan and M. Cakmak, *Macromolecules*, **38**, 2333 (2005), <https://doi.org/10.1021/ma048794f>

³⁷ Y. W. Han and C. D. Callihan, *Appl. Microbiol.*, **27**, 165 (1974), <https://doi.org/10.0000/PMID4809907>

³⁸ L. L. Zhou, D. P. Sun, L. Y. Hu, Y. W. Li and J. Z. Yang, *J. Ind. Microbiol. Biotechnol.*, **34**, 483 (2007), <https://doi.org/10.1007/s10295-007-0218-4>

³⁹ L. L. Zhou, D. P. Sun, Q. H. Wu, J. Z. Yang and S. L. Yang, *Acta Microbiol. Sin.*, **47**, 914 (2007), <https://doi.org/10.13343/j.cnki.wsxb.2007.05.012>

⁴⁰ A. Kljun, T. A. Benians, F. Goubet, F. Meulewaeter, J. P. Knox et al., *Biomacromolecules*, **12**, 4121 (2011), <https://doi.org/10.1021/bm201176m>

⁴¹ J. Gu and J. M. Catchmark, *Carbohyd. Polym.*, **88**, 547 (2012), <https://doi.org/10.1016/j.carbpol.2011.12.040>

⁴² W. Czaja, D. Romanowicz and R. M. Brown, *Cellulose*, **11**, 403 (2004), <https://doi.org/10.1023/b:cell.0000046412.11983.61>

- ⁴³ Y. A. Aydin and N. D. Aksoy, *Appl. Microbiol. Biot.*, **98**, 1065 (2013),
<https://doi.org/10.1007/s00253-013-5296-9>
- ⁴⁴ J. Bi, S. Liu, C. Li, J. Li, L. Liu *et al.*, *J. Appl. Microbiol.*, **117**, 1311 (2014),
<https://doi.org/10.1111/jam.12619>
- ⁴⁵ I. C. Um, C. S. Ki, H. Y. Kweon, K. G. Lee, D. W. Ihm *et al.*, *Int. J. Biol. Macromol.*, **34**, 119 (2004),
<https://doi.org/10.1016/j.ijbiomac.2004.03.011>